Progress In Electromagnetics Research Letter, Vol. 116, 23-30, 2024 PIER Letters

(Received 27 October 2023, Accepted 26 December 2023, Scheduled 30 December 2023)

Novel Sparse Linear Array Based on a New Suboptimal Number Sequence with a Hole-Free Difference Co-Array

Ashish Patwari[1,*] and Pradyumna Kunchala[2]

[1]*School of Electronics Engineering, Vellore Institute of Technology, Vellore, Tamil Nadu 632014, India*
[2]*Bachelor of Technology, Computer Science Engineering, Vellore Institute of Technology, Vellore, Tamil Nadu 632014, India*

ABSTRACT: In this paper, we propose a new sparse linear array (SLA) that enjoys a hole-free difference co-array (DCA) and closed-form expressions for its sensor positions. The proposed configuration is valid for arrays containing seven or more sensors ($N \geq 7$). Exact expressions for the array aperture and achievable degrees of freedom (DOFs) have been derived. Numerical simulations were performed using MATLAB to reinforce the theoretical understanding. The main aim of this study is not to claim superiority over any existing SLA design, but to report that we have found a new number sequence that can act as an SLA. Except for being highly susceptible to mutual coupling, the proposed array has all the desirable features of a good SLA. We observed that the proposed array is on par with other SLAs for $N < 20$. However, for 20 or more sensors, the array aperture does not scale rapidly in proportion to the added sensors and fails to match the resolution and/or DOFs offered by other sparse arrays. Nevertheless, the proposed sparse array is based on a unique and previously unknown number sequence.

1. INTRODUCTION

Sensor arrays have long been studied in various fields, such as radar, sonar, audio beamforming, chemical sensing, medical imaging, and wireless communications [1]. Sparse linear arrays (SLAs) are special sensor arrays capable of providing apertures on par with uniform linear arrays (ULAs) while requiring fewer sensors [2]. Consequently, SLAs provide huge savings in system costs and can aid in sustainable/green computing. The design of SLAs has received renewed attention in the past decade, given their ability to perform angle estimation in underdetermined cases (i.e., when there are more source angles to estimate than the number of sensors in the array) [3].

Sparse arrays are generally studied in the co-array domain. Co-array processing provides additional degrees of freedom (DOFs) that cannot be exploited if DOA estimation was to be performed directly on the physical array. DOFs refer to the number of detectable source angles. This process relies on the continuity of the co-array. For example, a sparse array with sensors at $\{0, 2, 5, 6\}$, normalized to half the wavelength, can generate all spatial lags (differences) from 0 to 6. This results in a difference set of $\{0, -1, -4, -6, 1, 0, -3, -5, 4, 3, 0, -2, 6, 5, 2, 0\}$. The difference set consists of all pairwise self- and cross-differences between the sensor locations in the physical array. The corresponding DCA is $\{-6, -5, -4, -3, -2, -1, 0, 1, 2, 3, 4, 5, 6\}$. Note that the repeating lag of zero from the difference set is considered only once.

Sparse linear arrays (SLAs), such as minimum redundancy array (MRA) and minimum hole array (MHA), were introduced in the 1960s and were primarily used for radio astronomy [4, 5]. MRAs and MHAs do not have closed-form expressions for sensor positions, and hence, exhaustive searching had to be employed to determine the optimum configurations. Coprime arrays have exact equations to determine the sensor positions but could not provide hole-free DCAs. In contrast, nested arrays provide hole-free DCAs along with closed-form expressions for sensor positions [6, 7]. The past decade (2010–2020) witnessed many novel sparse array designs, such as the super-nested array, augmented nested array, and improved nested array, to name a few [8–10]. A thorough review of the characteristics of various SLAs can be found in [11].

Many SLAs have been introduced in the past five years. Of these, the maximum inter-element spacing constraint (MISC) array is noteworthy [12]. The MISC array has received immediate and widespread attention from sparse array designers owing to its elegant formulation and immunity to mutual coupling. Although many SLAs were introduced after MISC, they either provide smaller apertures or are highly prone to mutual coupling. For example, the improved coprime nested array (ICNA), the ULA fitting with three base layers (UF-3BL), and the ULA fitting with four base layers (UF-4BL) have lower mutual coupling than MISC but cannot provide apertures as large as it does [13, 14].

On the other hand, the one-sided or two-sided extended nested array (OS/TS-ENA), the flexible extended nested array with multiple subarrays-I (f-ENAMS-I), the f-ENAMS-II, and the generalized extended nested array based on the MISC criterion (GENAMS) possess wider apertures than the MISC for a given number of sensors but are not as robust as the MISC against mutual coupling [15–17]. Although the improved MISC (IMISC) appears better than the MISC, it cannot provide a hole-free DCA [18]. Recently, the enhanced MISC (xMISC) has been introduced, which outperforms the classical

* Corresponding author: Ashish Patwari (ashish.p@vit.ac.in).

MISC both in terms of the aperture offered and immunity to mutual coupling [19].

Although many SLA configurations exist, none provide a fixed increment in the array aperture for each added sensor. For instance, consider an array of N sensors that can provide an aperture L. If this array can provide an aperture of $L+x$ with $N+1$ sensors and $L+2x$ with $N+2$ sensors, then it is said to have a fixed aperture increment of x units for each additional sensor. Such a property cannot be observed in existing SLAs. Therefore, we propose a novel SLA whose aperture follows an arithmetic progression with respect to the number of sensors. The proposed SLA is based on a naturally occurring number sequence that possesses almost all the properties desired for a good SLA. The proposed array can be designed instantly, as it has closed-form expressions for sensor positions. It also has a hole-free difference co-array. The proposed array is not superior to existing arrays in any sense. However, its formulation is based on a unique and previously unknown number sequence. The specific contributions of this paper are:

- A novel SLA configuration has been proposed based on a new number sequence. The specialty of this array is that its aperture follows an arithmetic progression for each additional sensor.
- Exact expressions for the array aperture and the DOFs offered have been derived.
- It is proved that the proposed array has a hole-free DCA.

Although the design of sparse arrays appears to be a mathematical problem on its surface (finding closed-form expressions for sensor positions such that the DCA is hole-free), it has many practical implications in real systems. There is a need to combine the antenna design, array synthesis, and array signal processing, as outlined in [20]. Advancements in the Internet of Things (IoT) and fifth-generation communication systems (5G) have enabled the existence of multiple tiny devices in a small area. Sidelobe level (SLL) minimization plays a major role in reducing interference between closely spaced devices [21–23]. Linear antenna arrays are widely used in mobile handsets and IoT devices. A slotted waveguide antenna array for indoor 5G applications was proposed in [24]. This approach essentially differs from microstrip or substrate-integrated waveguide (SIW) approaches, which are currently popular for antenna design [25–27].

The rest of the paper is organized as follows. Section 2 describes the relevant sparse array terminology. Section 3 describes the design of the proposed SLA. Section 4 discusses the numerical simulation results obtained using MATLAB. Section 5 lists the drawbacks of the proposed method. Section 6 concludes the paper with a few research directions.

2. BASIC SPARSE ARRAY TERMINOLOGY

This section briefly discusses the relevant sparse array terminology required to understand the ideas presented here.

2.1. Difference Co-Array

Consider an N-element linear array with physical sensors at $\mathbb{Z} = \{z_1, z_2, ..., z_N\}$, normalized to half the wavelength. The difference set $\mathbb{H}$ denotes all possible differences in $\mathbb{Z}$ (self- and cross-differences) and is given by

$$\mathbb{H} = \{z_i - z_j;\ \ i, j = 1, 2, ..., N\}. \tag{1}$$

Each entry in the difference set $\mathbb{H}$ is called a spatial lag. The sorted and nonrepeating entries of $\mathbb{H}$ form the difference co-array (DCA) $\mathbb{D}$. As the last sensor of $\mathbb{Z}$ is located at z_N its DCA should contain all spatial lags from $-z_N$ to $+z_N$ including zero. In short, $\mathbb{D}$ should be continuous from $[-z_N, z_N]$. A missing spatial lag forms a hole in the DCA. In general, hole-free DCAs are preferred because they aid in unambiguous DOA estimation. However, certain array types may contain holes in their DCAs. The set $\mathbb{U}$ denotes the central hole-free portion of $\mathbb{D}$. If the array is hole-free, then $\mathbb{D} = \mathbb{U}$.

2.2. Weight Function

The number of times a spatial lag appears in the difference set denotes its weight. The weight function lists the weights of all possible spatial lags in the DCA and is defined as follows:

$$w(m) = |\{(z_i, z_j);\ i, j = 1, 2, ..., N:\ z_i - z_j = m\}| \tag{2}$$

where $w(m)$ denotes the number of sensor pairs in the array with a separation of m (i.e., $m\lambda/2$). The function $|.|$ denotes the cardinality.

2.3. Signal Model

The signal model is based on coarray processing and is described in Appendix A as it is widely available in the existing literature.

3. THE PROPOSED SPARSE LINEAR ARRAY (SLA)

The proposed sparse array configuration for N sensors can be obtained by defining a scalar $p = N - 6$. The following number sequence denotes the sensor positions in the physical array (relative to half the wavelength)

$$\mathbb{S} = \Bigg\{ \overbrace{0, 1, 2, ..., p-1}^{ULA\ segment\ of\ p\ sensors},$$

$$\overbrace{(2p), (3p+2), (4p+4), (5p+4), (6p+5), (7p+5)}^{Last\ 6\ sensors\ that\ bestow\ sparsity} \Bigg\}. \tag{3}$$

Note that the proposed SLA configuration is valid for arrays containing seven or more sensors ($N \geq 7$, as proved shortly).

3.1. Array Aperture

It can be readily seen from (3) that the first sensor of the array lies at the origin, and the last sensor lies at $7p+5$. This gives an array aperture of

$$L = 7p + 5 = 7N - 37 \tag{4}$$

Based on (4), we can derive the smallest value of N that satisfies the sparse array configuration given by (3). The proposed SLA provides an aperture of $7N - 37$ for N sensors. On the other hand, a ULA with the same number of sensors can provide an aperture of only $N - 1$. If $\mathbb{S}$ in (3) were to denote a sparse array, the aperture L should exceed $N - 1$. By solving the inequality $7N - 37 > N - 1$, we find that the proposed SLA configuration in (3) is valid for $N > 6$. Hence, at least seven sensors are required to realize the proposed array.

One can also observe that the array aperture increases at a constant rate for each added sensor, i.e., there is a fixed increment of seven units of aperture for each added sensor. For instance, arrays with 16, 17, and 18 sensors provide apertures of 75, 82, and 89, respectively. It is rare to see SLAs whose apertures follow such arithmetic progressions. This feature of a fixed aperture increment is a boon for the array designer. Imagine a designer who wants an array with a half-power beamwidth/angular resolution of 5°. Then, as per the Rayleigh resolution limit ($\theta^{\circ}_{res} \cong 100/N$), an aperture of at least $L = 20$ is required. By solving (4), we find that $N = 9$ can provide the desired aperture. Now, consider another application that requires a resolution of 3°, which roughly corresponds to $L_{new} = 33$. The designer need not solve (4) again. Instead, as the difference between the two apertures is 13, it is sufficient to select an array that has two more sensors than the previous one, as each additional sensor provides an aperture increment of seven units.

3.2. DCA Span and DOFs Offered by the Proposed Array

The DCA of the proposed array would be hole-free from $[-L, L]$ (as proved next). Therefore, the DCA span $D = 2L + 1$ works out to be

$$D = 14N - 73 \tag{5}$$

In fact, D represents the DOFs of the proposed array. Moreover, because of the hole-free property of the proposed array, all DOFs essentially represent uniform DOFs. (uDOF).

Theorem: *The number sequence $\mathbb{S}$ in (3) generates a hole-free DCA.*

Proof:

1. Consider the ULA segment from 0 to $p-1$. This ensures that all spatial lags from 0 to $p - 1$ occur at least once.

2. Consider the sensor at $2p$. It causes $2p - \{0 : 1 : p - 1\}$, thereby resulting in new lags from $p + 1$ to $2p$. The difference 'p' can be obtained using the sensor pairs $(4p+4,\ 5p+4)$ and $(6p+5,\ 7p+5)$. Therefore, all spatial lags from 0 to 2p occur at least once.

3. Consider the sensor at $3p+2$. It causes $3p+2-\{0 : 1 : p-1\}$, thereby creating spatial lags from $2p+3$ to $3p+2$. The lag $2p+1$ can be generated from the sensor pairs $(4p+4,\ 6p+5)$ and $(5p+4,\ 7p+5)$. Similarly, the lag $2p+2$ can be generated using the sensor pair $(3p+2,\ 5p+4)$. Therefore, we now have all spatial lags from 0 to $3p + 2$.

4. Consider the sensor at $4p + 4$. It causes $4p + 4 - \{0 : 1 : p - 1\}$, thereby generating differences from $3p + 5$ to $4p + 4$. Remember that spatial lags until $3p + 2$ have been generatedin the previous steps. The lag $3p + 3$ can be generated using the sensor pair $(3p+2,\ 6p+5)$, whereas $3p+4$ can be generated using the sensor pair $(2p, 5p+4)$. In short, all spatial lags from 0 to $4p + 4$ have been generated at least onceuntil this point.

5. Consider the sensor at $5p + 4$. It causes $5p + 4 - \{0 : 1 : p - 1\}$ resulting in spatial lags from $4p + 5$ to $5p + 4$. By including the lags generated up to step 4, we have all lags from 0 to $5p + 4$.

6. Consider the sensor at $6p + 5$. It causes $6p + 5 - \{0 : 1 : p - 1\}$, thereby creating spatial lags from $5p + 6$ to $6p + 5$. We have all lags from 0 to $6p + 5$ except $5p + 5$. The sensor pair $(2p, 7p + 5)$ can generate the difference $5p + 5$. Hence, we obtain all lags from 0 to $6p + 5$.

7. Consider the last sensor at $7p+5$. This causes $7p+5-\{0 : 1 : p - 1\}$, thereby creating lags from $6p + 6$ to $7p + 5$. Considering the lags created until the previous step, all lags from 0 to $7p + 5$ have been generated at least once. Similarly, we can also obtain negative spatial lags from -1 to $-(7p+5)$ (by subtracting a higher position from a lower position). Essentially, we can say that D is continuous from $[-(7p + 5), (7p + 5)]$ or simply from $[-L, L]$, thereby proving the hole-free nature of the DCA. This completes the proof.

4. NUMERICAL SIMULATIONS

4.1. Array Examples with Weight Function

We start our discussion with $N = 7$, as this is the smallest value of N for which (3) represents an SLA. For $N = 7$, we get $p = 1$. Sensor positions were computed using (3) to obtain the array $\mathbb{S}_7 = \{0, 2, 5, 8, 9, 11, 12\}$. The corresponding weight function is shown in Fig. 1. As expected, all spatial lags have a weight of at least one, indicating the hole-free nature of the DCA.

As another example, Fig. 2 shows the weight function of a 12-element array, whose configuration can be obtained by substituting $p = 6$ in (3). The sensor positions are given by $\mathbb{S}_{12} = \{0, 1, 2, 3, 4, 5, 12, 20, 28, 34, 41, 47\}$. It can be observed that the first $N-6$ sensors follow the ULA format. Only the last six sensors produce the desired sparsity. It can be observed from Fig. 2 that the weight $w(0) = 12$. In fact, $w(0)$ for any array indicates the number of sensors.

4.2. DOF Ratio

In recent years, the parameter $\gamma(N)$ witnessed widespread usage to compare the DOF capacities of SLAs. $\gamma(N)$ is known as the DOF ratio of the array and is defined as

$$\gamma(N) = \frac{N^2}{\left(\frac{u\text{DOF} - 1}{2}\right)} \tag{6}$$

$\gamma(N)$ measures the redundant sensor pairs in the array with reference to the hole-free span of the co-array. A lower value of

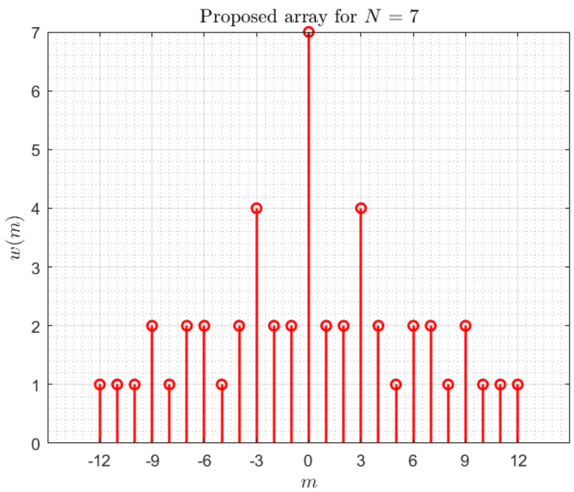

FIGURE 1. Weight function of the proposed array for $N = 7$.

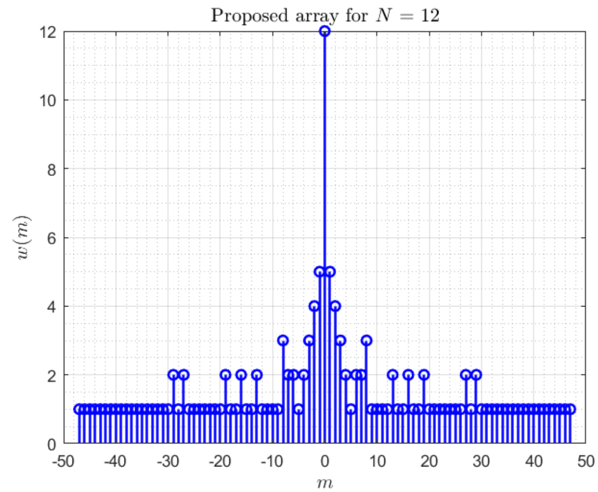

FIGURE 2. Weight function of the proposed array for $N = 12$.

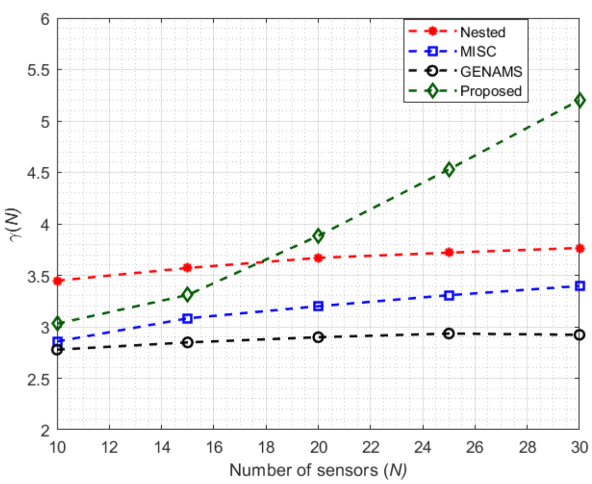

FIGURE 3. DOF ratios of SLAs considered in Table 1.

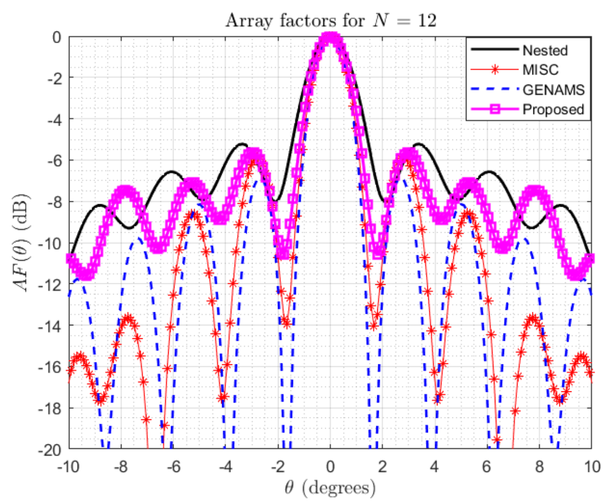

FIGURE 4. Array factors of SLAs listed in Table 2.

$\gamma(N)$ corresponds to larger apertures and higher DOFs. Because only SLAs with hole-free co-arrays have been considered in this study, we have $\left(\frac{u\text{DOF}-1}{2}\right) = L$ and $\gamma(N) = \frac{N^2}{L}$.

Next, we compared the values of $\gamma(N)$ versus N to observe how the proposed array compares with other SLAs. Table 1 lists the aperture L offered by a few well-known SLAs for different numbers of sensors. The SLAs in Table 1 are short listed based on the following reasoning: the nested array (NA) is the first SLA to have closed-form expressions for sensor positions along with a hole-free DCA [7]. The MISC array is a benchmark modern SLA because it provides a perfect balance between the achievable array aperture and immunity to mutual coupling [12]. The GENAMS array has the largest aperture among all SLAs (with closed-form expressions for sensor positions and a hole-free DCA) known to date [28].

Figure 3 shows the $\gamma(N)$ versus N values of the aforementioned arrays computed for each combination of N and L listed in Table 1. It can be observed from Fig. 3 that the proposed array is no different from the other arrays when $N < 20$. However, for $N > 20$, $\gamma(N)$ of the proposed array starts to increase rapidly as its aperture does not scale in proportion to the number of added sensors.

4.3. Radiation Pattern of SLAs

Next, we compare the radiation pattern of the proposed array with those of the other SLAs mentioned above. Sparse arrays provide poorer sidelobe rejection than ULAs with the same apertures. However, it would be interesting to study how they compare within themselves. As known, the radiation pattern gives a measure of the array's directivity and sidelobe suppression ability. Toward this end, we noted the array configurations of the nested array, MISC array, GENAMS array, and the proposed array for $N = 12$ in Table 2 and computed the respective array factors using MATLAB. The formula for computing the array factor is provided in Appendix B.

Figure 4 shows the array factors for the SLA configurations listed in Table 2. Minor variations exist in the sidelobe levels (SLLs) and main lobe widths (beamwidths) offered by differ-

TABLE 1. Apertures offered by a few well-known SLAs with hole-free DCAs.

	Aperture L			
N	Nested array	MISC	GENAMS	Proposed
10	29	35	36	33
15	63	73	79	68
20	109	125	138	103
25	168	189	213	138
30	239	265	308	173

TABLE 2. Array configurations of various SLAs for $N = 12$.

Type of SLA	Sensor positions relative to $\lambda/2$
Nested Array	[0, 1, 2, 3, 4, 5, 6, 13, 20, 27, 34, 41]
MISC array	[0, 1, 6, 14, 22, 30, 38, 40, 42, 45, 47, 49]
GENAMS array	[0, 1, 3, 6, 13, 20, 27, 34, 41, 45, 49, 50]
Proposed Array	[0, 1, 2, 3, 4, 5, 12, 20, 28, 34, 41, 47]

TABLE 3. Array configurations of various SLAs for $N = 18$.

SLA type	Sensor positions relative to $\lambda/2$
Nested Array	[0, 1, 2, 3, 4, 5, 6, 7, 8, 9, 19, 29, 39, 49, 59, 69, 79, 89]
MISC array	[0, 1, 8, 18, 28, 38, 48, 58, 68, 78, 88, 90, 92, 94, 97, 99, 101, 103]
GENAMS array	[0, 1, 2, 5, 10, 15, 26, 37, 48, 59, 70, 81, 92, 98, 104, 110, 111, 112]
Proposed Array	[0, 1, 2, 3, 4, 5, 6, 7, 8, 9, 10, 11, 24, 38, 52, 64, 77, 89]

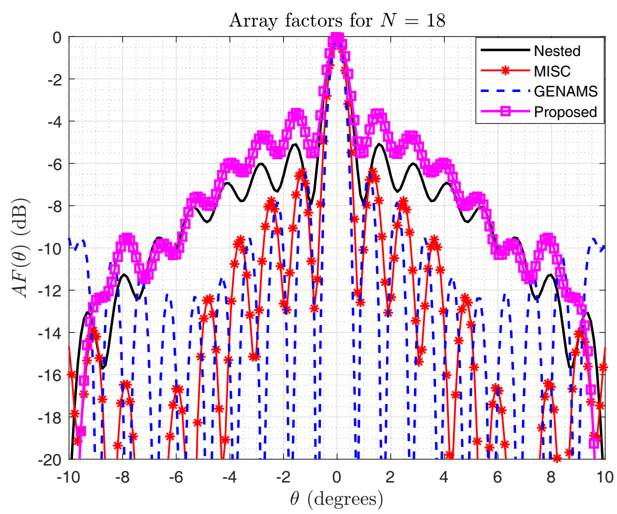

FIGURE 5. Array factors of SLAs listed in Table 3.

ent arrays. Upon careful examination, it can be observed that the proposed array, MISC array, and GENAMS array provide sharper radiation characteristics than the nested array, both in terms of the main lobe width and peak SLLs. This is understandable because the nested array has a slightly smaller aperture than other arrays for $N = 12$. However, it should be noted that Fig. 4 is a zoomed version of the radiation pattern and covers only $[-10^\circ, 10^\circ]$ of the angular spectrum. If we consider the full angular spectrum, these variations are negligible.

To obtain further insights into the radiation characteristics of the above SLAs, we computed their array factors for $N = 18$. Table 3 lists the array configurations and Fig. 5 shows the respective array factors. It can be observed that the MISC and GENAMS arrays provide sharper main beams and better sidelobe rejection than the proposed array owing to the broader apertures that they possess.

Of significant interest in Fig. 5 is the difference between the radiation patterns of the nested and proposed arrays. Both these arrays provide an aperture of 89 for $N = 18$, as listed in Table 3.

Even with the same aperture and number of sensors, the nested array exhibited better sidelobe characteristics than the proposed array. Hence, it can be inferred that the radiation pattern of sparse arrays is a function of the array configuration and not just the aperture. Similar results have been reported for minimum redundancy arrays (MRAs) in the past. Array factors of four MRAs, each with seven sensors and an aperture of 15, were compared [11]. It was found that the sensitivity of the array was based on the position of the sensors within the aperture.

It can be observed from Figs. 4 and 5 that the proposed array has radiation characteristics that are comparable to those of the other SLAs. The main lobe widths almost the same. However, the arrays differed in their sidelobe characteristics.

5. LIMITATIONS

Although the proposed array has almost all desirable properties of SLAs, the fact that there is a dense ULA segment with $N-6$ sensors at the beginning of the array makes it vulnerable to mutual coupling. The weight $w(1)$ is often used to in the analysis of sparse arrays because it empirically determines the array's robustness to mutual coupling. The proposed array has $N-7$ sensor pairs with unit spacing; hence, $w(1)=N-7$. This value is high, indicating that the array is highly susceptible to mutual coupling. For comparison, the two-level nested array has $w_{NA}(1) \cong N/2$. Other sparse arrays, such as the coprime array, super-nested array, augmented nested array, and minimum redundancy array, possess lower values for $w(1)$ and are therefore less prone to mutual coupling. The MISC array is least susceptible to mutual coupling because it has only one sensor pair with unit spacing, i.e., $w_{\text{misc}}(1)=1$.

Another drawback of the proposed array is that its aperture does not scale exponentially with the number of sensors used. Consequently, it fails to match the DOFs offered by the aforementioned sparse arrays for $N \geq 20$. For example, a 40-element nested array provides an aperture of 419, whereas the proposed array provides only an aperture of 243 for the same number of sensors.

6. CONCLUSION AND FUTURE SCOPE

A new number sequence is proposed that can serve as a sparse linear array with a hole-free DCA and closed-form expressions for sensor positions. Numerical simulations conclude that the proposed array matches the apertures and DOFs offered by other well-known sparse arrays when there are fewer than 20 sensor elements. Another notable feature of the proposed SLA is the fixed increment in its aperture for each added sensor, a property that is rarely observed in sparse arrays. It should be noted that the array is highly prone to mutual coupling. However, the novel configuration and straightforward formulation of the array outweigh these limitations.

Future scope involves modifying the array configuration by relocating a few sensors from the dense ULA portion to other positions with the aim of reducing the weight $w(1)$. The same logic was employed in the past to design super-nested arrays and augmented nested arrays from two-level nested arrays to reduce mutual coupling [8, 9].

Another extension of this study is to explore new number sequences that can generate sparse arrays robust to single-element failures. Such arrays have sensors at specified positions to ensure that all spatial lags from 0 to $L-1$ occur at least twice. The DCA of such arrays remains intact (hole-free) even when one of the sensors fails. Such new arrays can act as sub-optimal versions of robust minimum redundancy arrays (RMRAs),as envisaged by Liu and Vaidyanathan [29].

APPENDIX A.

The procedure for DOA estimation in SLAs using the co-array MUSIC algorithm is explained here. An SLA containing N sensor elements is considered. It is assumed that it offers an aperture of L units ($L > N$). The sparse array is laid out on a linear grid where each grid point is an integer multiple of the basic unit of inter-element spacing, namely, $d=\lambda/2$. In other words, the locations of the sensors are normalized to half of the wavelength. K narrowband sources with powers $\{\sigma_i^2;\, i = 1 \,\text{to}\, K\}$ impinge the array from the angles $\{\theta_i;\, i = 1 \,\text{to}\, K\}$. The signal received by the array at the lth time instant or snapshot is given by the $N \times 1$ column vector

$$\mathbf{x}\left(l\right) = \mathbf{A}\mathbf{s}\left(l\right) + \mathbf{n}\left(l\right) \tag{A1}$$

where $s(l)$ is the $K \times 1$ column vector of incoming complex narrowband signals and is given by $\mathbf{s}(l) = [s_1(l)\ s_2(l)\ ...\ s_K(l)]^T$, and the $N \times 1$ vector $\mathbf{n}(l)$ denotes the noise at each array element. The noise has a zero mean and variance σ_n^2. $\mathbf{A} = [\mathbf{a}(\theta_1)\ \mathbf{a}(\theta_2)\ \cdots\ \mathbf{a}(\theta_K)]$ is a $N \times K$ array manifold matrix whose columns $\mathbf{a}(\theta_i)$; $i = 1, 2, ..., K$ denote the steering vector for a particular direction θ_i. Sources are assumed to be uncorrelated; therefore, the source covariance matrix $\mathbf{R}_{ss}$ is diagonal. The entries in the individual vectors $\mathbf{a}(\theta_i)$ are given by

$$\mathbf{a}\left(\theta_i\right) = \left[e^{-jkz_1 \sin\theta_i},\ e^{-jkz_2 \sin\theta_i},\ e^{-jkz_3 \sin\theta_i},\right. \\ \left. ...,\ e^{-jkz_N \sin\theta_i}\right]^T \tag{A2}$$

where the set $\mathbb{Z} = \{z_1,\ z_2,\ ...,\ z_N\}$ indicates the positions of the sensors in the linear sparse array. More specifically, the first sensor lies at the origin and the last sensor lies at the grid point Ld. The array correlation matrix is given by

$$\mathbf{R}_{xx} = \mathbf{A}\mathbf{R}_{ss}\mathbf{A}^H + \mathbf{R}_{nn} \tag{A3}$$

where $\mathbf{R}_{ss}$ denotes the $K \times K$ source correlation matrix, and $\mathbf{R}_{nn}$ denotes the $N \times N$ noise correlation matrix. For sparse arrays, further processing steps are required before the correlation matrix can be subjected to eigenvalue decomposition (EVD). Given the missing sensors in the physical array, its correlation matrix does not have all spatial lags. As a result, the array correlation matrix is incomplete and does not represent a Toeplitz structure. Hence, the analysis is shifted to the coarray domain. To formulate the problem in the coarray domain, the correlation matrix $\mathbf{R}_{xx}$ has to be vectorized using the procedure given in [30] to form a new vector $\mathbf{y}$ of size $N^2 \times 1$ given by

$$\mathbf{y} = \text{vec}\left(\mathbf{R}_{xx}\right) = \mathbf{B}\mathbf{c} + \sigma_n^2\mathbf{i} \tag{A4}$$

where $\mathbf{c} = \left[\sigma_1^2, \sigma_2^2, \cdots, \sigma_K^2\right]^T$ and $\mathbf{i} = \text{vec}(\mathbf{I}) = \left[\mathbf{e}_1^T, \mathbf{e}_2^T, \cdots, \mathbf{e}_N^T\right]^T$, with $\mathbf{e}_i$ being a column vector of all zeros except a one at the ith position. $\mathbf{B} = [\mathbf{b}(\theta_1)\ \mathbf{b}(\theta_2)\ \cdots\ \mathbf{b}(\theta_P)]$ denotes the manifold matrix of an augmented imaginary array, whose sensors are located at the positions given by the difference set $\mathbb{H}$ of the sparse array. The individual columns of $\mathbf{B}$ denote the steering vectors $\mathbf{b}(\theta_i) = \mathbf{a}^*(\theta_i) \otimes \mathbf{a}(\theta_i)$ of size $N \times 1$. The symbol $\otimes$ denotes the Kronecker product. The entries $\mathbf{a}^*(\theta_i) \otimes \mathbf{a}(\theta_i)$ are of the form $\{e^{-jk(z_i - z_j)\sin\theta_i}; i, j = 1, 2, ..., N\}$ where an individual entry represents the phase of the signal received by a sensor positioned at $z_i - z_j$. In short, $\mathbf{y}$ resembles the signal received at the difference set array whose manifold is $\mathbf{B} = \mathbf{A}^* \odot \mathbf{A}$. The symbol $\odot$ denotes the Khatri-Rao (KR) product. The equivalent source signal vector is given by $\mathbf{c}$ and noise is given by $\sigma_n^2\mathbf{i}$.

Because the unique and sorted entries in the difference set constitute the difference co-array (DCA), the unique and sorted rows of $\mathbf{A}^* \odot \mathbf{A}$, denoted by $\tilde{\mathbf{B}}$, correspond to the DCA manifold.

$$\tilde{\mathbf{y}} = \text{unique}(\mathbf{y}) = \tilde{\mathbf{B}}\mathbf{c} + \sigma_n^2\mathbf{i} \tag{A5}$$

Here, $\tilde{\mathbf{y}}$ represents the signal received at the DCA. Hence, instead of $\mathbf{x} = \mathbf{A}\mathbf{s} + \mathbf{n}$, the data in $\tilde{\mathbf{y}} = \tilde{\mathbf{B}}\mathbf{c} + \sigma_n^2\mathbf{i}$ could be used for DOA estimation. That is, the DCA can be used for DOA estimation in place of physical SLA. This is the essence of sparse array processing where the data are converted to second-order spatial statistics. For a sparse array with an aperture L, the DCA spans from $-L$ to L provided that it is hole-free. To perform DOA estimation using the co-array MUSIC algorithm, the correlation matrix of the signal received at the DCA is needed. The data in $\tilde{\mathbf{y}}$ could be represented as a Hermitian Toeplitz matrix structure to obtain the co-array correlation matrix as follows:

$$\mathbf{R}_{yy} = \begin{bmatrix} \tilde{y}_0 & \tilde{y}_{-1} & \cdots & \tilde{y}_{-L} \\ \tilde{y}_1 & \tilde{y}_0 & & \tilde{y}_{-(L-1)} \\ \vdots & & \ddots & \vdots \\ \tilde{y}_L & \tilde{y}_{L-1} & \cdots & \tilde{y}_0 \end{bmatrix} \tag{A6}$$

where $\tilde{y}_i$ denotes the ith entry of $\tilde{\mathbf{y}}$. The matrix $\mathbf{R}_{yy}$ is a full rank matrix and can therefore be used to estimate the DOAs through subspace decomposition. The remaining procedure is similar to the conventional MUSIC algorithm, in which the correlation matrix is subjected to EVD to form the signal and noise subspaces. The pseudospectrum is then calculated using the conventional MUSIC procedure.

APPENDIX B.

As per the principle of pattern multiplication, the overall array response is the product of the element pattern and the array factor. Considering point sources with isotropic pattern, the far field pattern is just a function of the array factor which is given by

$$\text{AF}(\theta) = \frac{1}{N}\sum_{n=1}^{N} e^{-jks_n \sin\theta} \tag{B1}$$

where $k = \frac{2\pi}{\lambda}$ denotes the wavenumber, and N is the number of array elements, θ = azimuth angle, $0^\circ \leq \theta \leq 180^\circ$. The set $\mathbb{S}$ denotes sensor positions of the sparse array in terms $d = \lambda/2$. Likewise, s_n denotes the position of the nth sensor in terms of d. For instance, the set $\mathbb{S} = [0, 1, 4, 6]$ actually denotes sensors at $[0d, 1d, 4d, 6d]$. Accordingly, s_3 refers to the third sensor in $\mathbb{S}$ and $s_3 = 4d$ goes into (B1).

REFERENCES

[1] Monzingo, R. A., R. L. Haupt, and T. W. Miller, *Introduction to Adaptive Arrays*, 2nd ed., Institution of Engineering and Technology, 2011.

[2] Van Trees, H. L., *Detection, Estimation, and Modulation Theory, Optimum Array Processing*, John Wiley & Sons, 2004.

[3] Liu, C.-L. and P. P. Vaidyanathan, "Cramér-Rao bounds for coprime and other sparse arrays, which find more sources than sensors," *Digital Signal Processing*, Vol. 61, 43–61, Feb. 2017.

[4] Moffet, A. T., "Minimum-redundancy linear arrays," *IEEE Transactions on Antennas and Propagation*, Vol. 16, No. 2, 172–175, Mar. 1968.

[5] Meyer, C. and P. A. Papakonstantinou, "On the complexity of constructing Golomb rulers," *Discrete Applied Mathematics*, Vol. 157, No. 4, 738–748, Feb. 2009.

[6] Vaidyanathan, P. P. and P. Pal, "Sparse sensing with co-prime samplers and arrays," *IEEE Transactions on Signal Processing*, Vol. 59, No. 2, 573–586, Feb. 2010.

[7] Pal, P. and P. P. Vaidyanathan, "Nested arrays: A novel approach to array processing with enhanced degrees of freedom," *IEEE Transactions on Signal Processing*, Vol. 58, No. 8, 4167–4181, Aug. 2010.

[8] Liu, C.-L. and P. P. Vaidyanathan, "Super nested arrays: Linear sparse arrays with reduced mutual coupling — Part I: Fundamentals," *IEEE Transactions on Signal Processing*, Vol. 64, No. 15, 3997–4012, Aug. 2016.

[9] Liu, J., Y. Zhang, Y. Lu, S. Ren, and S. Cao, "Augmented nested arrays with enhanced DOF and reduced mutual coupling," *IEEE Transactions on Signal Processing*, Vol. 65, No. 21, 5549–5563, Nov. 2017.

[10] Yang, M., L. Sun, X. Yuan, and B. Chen, "Improved nested array with hole-free DCA and more degrees of freedom," *Electronics Letters*, Vol. 52, No. 25, 2068–2070, Dec. 2016.

[11] Patwari, A., "Sparse linear antenna arrays: A review," *Antenna Systems*, IntechOpen, 2021.

[12] Zheng, Z., W.-Q. Wang, Y. Kong, and Y. D. Zhang, "MISC array: A new sparse array design achieving increased degrees of freedom and reduced mutual coupling effect," *IEEE Transactions on Signal Processing*, Vol. 67, No. 7, 1728–1741, Apr. 2019.

[13] Shi, W., S. A. Vorobyov, and Y. Li, "ULA fitting for sparse array design," *IEEE Transactions on Signal Processing*, Vol. 69, 6431–6447, 2021.

[14] Peng, Z., Y. Ding, S. Ren, H. Wu, and W. Wang, "Coprime nested arrays for DOA estimation: Exploiting the nesting property of coprime array," *IEEE Signal Processing Letters*, Vol. 29, 444–448, 2022.

[15] Wandale, S. and K. Ichige, "Flexible extended nested arrays for DOA estimation: Degrees of freedom perspective," *Signal Processing*, Vol. 201, 108710, Dec. 2022.

[16] Wandale, S. and K. Ichige, "A generalized extended nested array design via maximum inter-element spacing criterion," *IEEE Signal Processing Letters*, Vol. 30, 31–35, 2023.

[17] Ren, S., W. Dong, X. Li, W. Wang, and X. Li, "Extended nested arrays for consecutive virtual aperture enhancement," *IEEE Signal Processing Letters*, Vol. 27, 575–579, 2020.

[18] Shi, W., Y. Li, and R. C. de Lamare, "Novel sparse array design based on the maximum inter-element spacing criterion," *IEEE Signal Processing Letters*, Vol. 29, 1754–1758, 2022.

[19] Wandale, S. and K. Ichige, "xMISC: Improved sparse linear array via maximum inter-element spacing concept," *IEEE Signal Processing Letters*, Vol. 30, 1327–1331, 2023.

[20] Patwari, A. and G. R. Reddy, "A conceptual framework for the use of minimum redundancy linear arrays and flexible arrays in future smartphones," *International Journal of Antennas and Propagation*, Vol. 2018, No. 9629837, 12, 2018.

[21] Lema, G. G., D. H. Hailu, and T. B. Wuneh, "SLL attenuation-based thinned antenna design for next-generation communications," *EURASIP Journal on Wireless Communications and Networking*, Vol. 2019, No. 1, 225, Sep. 2019.

[22] Buttazzoni, G., F. Babich, F. Vatta, and M. Comisso, "Geometrical synthesis of sparse antenna arrays using compressive sensing for 5G IoT applications," *Sensors*, Vol. 20, No. 2, Art. no. 2, Jan. 2020.

[23] Hasan, M. Z. and H. Al-Rizzo, "Beamforming optimization in internet of things applications using robust swarm algorithm in conjunction with connectable and collaborative sensors," *Sensors*, Vol. 20, No. 7, Art. no. 7, Jan. 2020.

[24] Sodré, A. C., I. F. d. Costa, R. A. d. Santos, H. R. D. Filgueiras, and D. H. Spadoti, "Waveguide-based antenna arrays for 5G networks," *International Journal of Antennas and Propagation*, Vol. 2018, May 2018.

[25] Chaturvedi, D., A. Kumar, and A. A. Althuwayb, "A dual-band dual-polarized SIW cavity-backed antenna-duplexer for off-body communication," *Alexandria Engineering Journal*, Vol. 64, 419–426, Feb. 2023.

[26] Chaturvedi, D. and A. Kumar, "A QMSIW cavity-backed self-diplexing antenna with tunable resonant frequency using CSRR slot," *IEEE Antennas and Wireless Propagation Letters*, 1–5, 2023.

[27] Chaturvedi, D., A. Kumar, A. A. Althuwayb, and F. Ahmadfard, "SIW-backed multiplexing slot antenna for multiple wireless system integration," *Electronics Letters*, Vol. 59, No. 11, e12826, Jun. 2023.

[28] Wandale, S. and K. Ichige, "A generalized extended nested array design via maximum inter-element spacing criterion," *IEEE Signal Processing Letters*, Vol. 30, 31–35, 2023.

[29] Liu, C.-L. and P. P. Vaidyanathan, "Optimizing minimum redundancy arrays for robustness," in *2018 Conference Record of 52nd Asilomar Conference on Signals, Systems, and Computers*, 79–83, Oct. 2018.

[30] Ma, W.-K., T.-H. Hsieh, and C.-Y. Chi, "DOA estimation of quasi-stationary signals via Khatri-Rao subspace," in *2009 IEEE International Conference on Acoustics, Speech, and Signal Processing*, 2165–2168, Apr. 2009.